17th World Conference on Earthquake Engineering, 17WCEE
Sendai, Japan - September 13th to 18th 2020

ECCENTRICALLY BRACED BEAM-THROUGH STEEL FRAMES WITH REPLACEABLE SHEAR LINKS: CYCLIC TESTING

Z. Yao[(1)], W. Wang[(2)]

[(1)] *PhD student, State Key Laboratory of Diaster Reduction in Civil Engineering, Tongji University, yaozucheng@tongji.edu.cn*
[(2)] *Professor, State Key Laboratory of Diaster Reduction in Civil Engineering, Tongji University, weiwang@tongji.edu.cn*

Abstract

Prefabricated tension-only concentrically braced beam-through frames (BTFs) have been popularized for low-rise steel buildings in low to moderate seismic regions. However, the energy dissipation capability of such system under earthquakes is limited due to the deteriorating pinched hysteretic behavior of the tension-only concentric braces. This study presents a new type of eccentrically braced lateral force-resisting system aiming to provide enhanced energy dissipation capability for BTFs, and in addition, seismic resilience is promoted with the utilization of replaceable shear link beams as structural fuses. In this paper, the specific configuration of the new eccentrically braced BTFs is first illustrated via introducing the basic design concept. The essential mechanical characteristics of the bracing system are subsequently described with a simplified theoretical model. This is followed by an experimental investigation on a full-scale BTF with seven different eccentric brace specimens which are designed to reveal the influences of three structural parameters, i.e., link length, bracing angle and link section. The global hysteretic behavior of the frame and the local behavior of the links in the different specimens are illustrated and discussed. Finally, a comparative analysis based on the test results is conducted. The tests show that short links tend to improve the stiffness, load resistance and ductility of the BTF due to the exhibited shear-dominant behavior. An increase in bracing angle leads to increased lateral stiffness and load resistance of the BTF but at the cost of reduced ductility. Reducing the link section helps delay the development of weld cracks and results in better ductility of the structural fuse. The test results also warn that weld defects and inappropriate design of the link beam could induce brittle weld fractures at the ends of the link.

Keywords: eccentrically braced frames, beam-through frames, replaceable shear links, seismic resilience, cyclic test.

1. Introduction

In responds to building industrialization, a new type of prefabricated structural system, termed as beam-through frames (BTFs) [1], was presented and is now gaining increasing popularity for low-rise buildings in many countries such as China and Japan. As illustrated in Fig. 1, fundamental components of this system, which are manufactured in factories and transported to the construction site for assembly, typically include discontinuous cold-formed square tube or H-section columns, H-section through beams, and tension-only slender concentric braces (TOCBs). Besides the merits of improved quality and increased speed for construction, BTFs adopt the strategy of controlling damage to achieve desirable seismic performance. The strong-beam-weak-column main frame, which is composed of discontinuous columns and through beams with simple or semi-rigid bolted connections, basically serve as gravity-resisting system and is designed to remain elastic under seismic loading, while TOCBs are applied to bear nearly all lateral forces. This kind of lateral force-resisting system is sufficient for normal design loads such as wind load. Under seismic conditions, however, the TOCBs exhibit elongation in tension but buckling in compression. Although such behavior may result in small overall residual displacement and allows quick seismic rehabilitation as damage is concentrated in the braces, the consequent deteriorating pinching action leads to compromised stiffness and energy dissipation of the BTF system, and increases the risk of structural collapse especially during severe earthquakes.

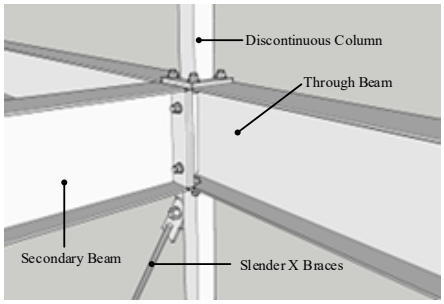

Fig. 1 – Fundamental components of EBFs

Further researches, where improvements were primarily focused on seismic loading-resisting system, were conducted to overcome these shortcomings of EBFs. Self-centering modular panels (SCMPs) [2] that refer to modules of posttensioned (PT) steel moment-resisting frame was developed to enhance the self-centering ability of BTFs. Meanwhile, additional lateral stiffness of SCMPs mitigate the possibility of soft-story mechanism for BTFs because of eliminating the zero initial stiffness associated with yielded TOCBs. However, energy dissipation contributed by TOCBs was still limited. Attempts to increase the energy dissipation capacity of BTFs were made with the utilization of slit steel plate shear walls (SWs) [3] on the basis of SCMPs. Nevertheless, the resulting pinching hysteresis behavior of SWs was quite similar with TOCBs, which was suitable for realizing seismic resilience. Therefore, other alternative methods to enable post-earthquake rehabilitation of BTFs, such as replacing the structural fuses after earthquakes, and improved lateral force-resisting systems with stable and controllable plastic deformation, could be better choices with the consideration of sufficient energy dissipation.

Apart from the conventional concentrically braced frames (CBFs), eccentrically braced frames (EBFs) are alternative solutions enabling enhanced hysteretic energy absorption capacity while ensuring sufficient lateral stiffness [4]. Of EBF systems, a critical beam segment called a “link”, is designed as the structural fuse to dissipate large amounts of input energy under severe earthquakes through the concentrated plastic deformation. Previous extensive experimental studies on link beams subjected to cyclic loading reveal that short links with shear-dominant behavior have considerably better performance in terms of strength and ductility than long links with flexure-dominant behavior [5-7]. In order to further realize rapid seismic rehabilitation of EBFs, the concept of replaceable links [8] that refers to decoupling the link beams from the floor beams was proposed and received significant attentions. Additionally, replaceable link beams have also been promoted for other structural systems such as linked column frames and coupled wall systems with the

advantages of stable behavior and easy construction. With respect to assembly, these replaceable fuses are often installed via web-bolted connection or bolted endplate connections [9]. Although the former makes the installation and replacement of links more practical, extra reinforcing details are necessary to overcome the pinching hysteretic behavior caused by bolt-slip under repeated loading cycles. For the latter, the link beams are welded to the end-plate that is then bolted to the main frame, which is relatively simple.

Web fractures, which are initiated by web buckling in links without web stiffeners and induced by stress concentrations of welds connecting intermediate stiffeners to the web in links with web stiffeners [10-12], are commonly observed for link beams under cyclic loading. However, this ductile failure mode will not occur in absence of effective end connections. In practice, failure of bolted endplate connections is sometime predominant by the matter of weld cracking in link-to-endplate interface [13,14], which is quite undesirable. Thus, complete joint penetration (CJP) welds and partial joint penetration (PJP) welds, rather than fillet welds, are mainly used for the fabrication of the link endplates in order to avoid early failure in the welded region [9,14]. Furthermore, considering stress concentrations in welded region and inconsistent qualities of welding technology, the ductility of the links could be better ensured using reduced link sections [15] or end stiffeners [16].

In the light of previous discussions, a new seismic system, namely, eccentrically braced beam-through steel frames (EBBTFs), was proposed. The new system employs replaceable shear links as the structural fuses for the beam-through main frames. On one hand, these links provide more stable and reliable energy dissipation than the TOCBs and SWs used presently. On the other hand, with damage restricted to the structural fuses, residual displacement may still be eliminated through replacing the structural fuses after earthquakes, which encourages expedited recovery of functionality after earthquakes. This study aims to investigate the seismic performance of EBBTFs with replaceable links under cyclic lateral loading. The working mechanisms of the newly proposed systems are presented first, followed by a comprehensive experimental study. The tests consist of seven full-scale of eccentric brace specimens to examine influence of the length of links, the angle of braces and the section feature of links. The failure mode, hysteretic behavior, lateral stiffness and ductile yielding capacity of these specimens were particularly discussed, and a comparative analysis was conducted to draw several conclusions for preliminary design recommendation.

2. Conceptual Design

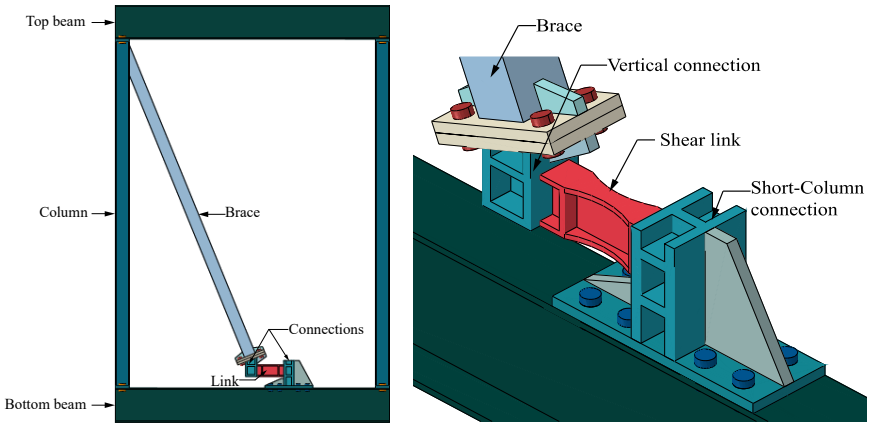

Fig. 2 – Typical structural form of EBBTFs

As illustrated in Fig. 2, the newly proposed EBBTFs typically consist of two parts, the floor-by-floor assembled beam-through steel main frames and the eccentric braces. The structural fuses, shear link beams are horizontally placed independently outside of the floor beam, which is derivative from the concept of the vertical links. This new eccentric bracing is not only suitable of assembly in BTFs, but also enable the undamaged state of the floors under earthquakes and benefit the easy installation and post-earthquake

rehabilitation. Bolted endplate connections which are still further convenient for rapid construction and seismic repair process, are widely utilized in this system, covering the beam-to-column connections, the link-to-brace connections and the link-to-beam connections. The vertical connection and the short-column connection are welded respectively to the two ends of shear links, conjointly forming the crucial replaceable components of this seismic structural system. Besides, the braces are welded to the columns. In order to avoid the early brittle failure induced by the existence of welding defects and complex residual stress, the aforementioned idea of reduced link sections is applied and the flanges of shear links are trimmed into "dog-bone" shape.

3. Theoretical Behavior

To alleviate the lateral resistant force of the columns and to enlarge the deformation of links under seismic loading, non-extended bolted endplate connections with just a row of bolts are applied to the through-beam-to-column connections, which are reasonable to be assumed as hinge connections. Therefore, the simplified theoretical analysis model is proposed as Fig. 3, with ignoring the large-stiffness vertical connection and short-column connection. Consequently, the mechanical characteristics of the EBBTFs can be described in terms of the column height H, bracing angle α, bracing length L, link length e and sectional features of each components.

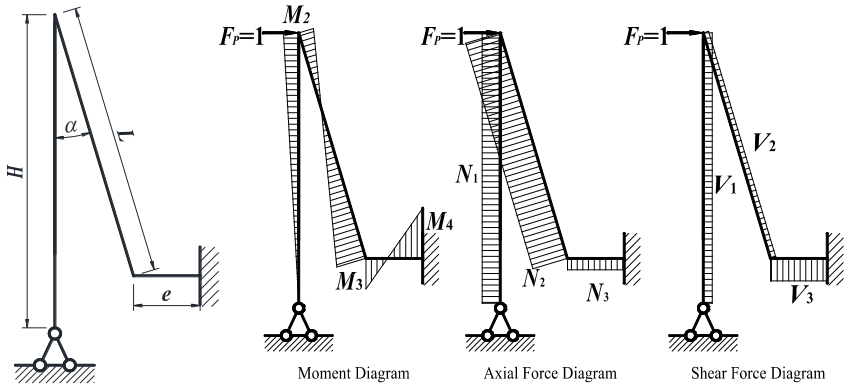

Fig. 3 – Simplified theoretical analysis model of the lateral force-resisting system of EBBTFs

3.1 Distribution of internal force

Through the force method of structural mechanics, the distribution of internal forces of the statically indeterminate structure subjected to unit lateral load, can be obtained and is showed in Fig. 3. It is clear that under lateral load the links carry large end moments, large shear forces and relatively minor axial forces, similar with the traditional EBFs. Hence, to ensure the shear-dominant behavior, the length of the links e need to be limited below $1.6M_p/V_p$ [17], where M_p and V_p are the plastic moment and plastic shear capacities of the links.

3.2 Elastic stiffness and yield capacity

From the deformation of the EBBTF under lateral load shown in Fig. 4(a), it is obvious that the lateral displacement of the EBBTF under unit lateral load contributed by five parts:

(1) Δ_1, lateral displacement caused by axial deformation of the columns;

(2) Δ_2, lateral displacement caused by axial deformation of the braces;

(3) Δ_3, lateral displacement caused by bending moment deformation of the braces;

(4) Δ_4, lateral displacement caused by shear deformation of the links;

(5) Δ_5, lateral displacement caused by bending moment deformation of the links.

Each of the parts can be determined by the formulation (1) -(5),

$$\Delta_1 = \frac{N_1^2 H^2}{EA_c} \tag{1}$$

$$\Delta_2 = \frac{N_2^2 L^2}{EA_b} \tag{2}$$

$$\Delta_3 = \frac{M_2^2 L - M_2 M_3 L + M_3^2 L}{3EI_b} \tag{3}$$

$$\Delta_4 = \frac{k_l V_3^2 e}{GA_l} \tag{4}$$

$$\Delta_5 = \frac{M_3^2 e + M_3 M_4 e + M_4^2 e}{3EI_l} \tag{5}$$

where M_i, N_i and V_i are the internal forces at the joints of the simplified model under unit lateral force (see Fig. 3); H, L and e are the length of column, brace and link respectively; A_c, A_b and A_l are the sectional area of the column, brace and link respectively; E is Young's modulus and G is the shear modulus; k_l is coefficient of uniformity resulted from the nonuniform distribution of shear stress.

Thus, the lateral elastic stiffness of this system K can be calculated with

$$K = 1 \Big/ \sum_{i=1}^{5} \Delta_i \tag{6}$$

Assuming the column and the brace as axial-force elements, the lateral yield load F_p for EBBTF with shear link is simply and conservatively defined as

$$F_p = V_p \tan\alpha \tag{7}$$

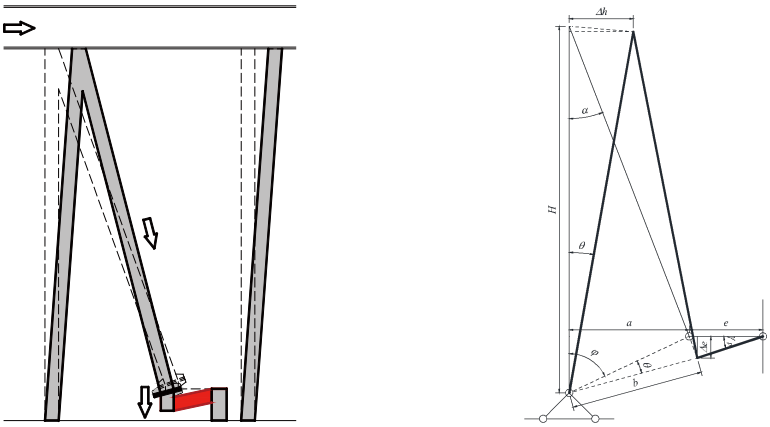

(a) Deformation of components (b) Deformation mechanism with rigid-plastic analysis

Fig. 4 – Deformation of the EBBTF under lateral load

3.3 Deformation mechanism

As to get the ductility demand of the structural fuses-shear links at the preliminary design stage, a rigid plastic mechanism that ignores the elastic deformation, is used to estimate the inelastic link rotation angle [18]. Kinematically admissible field of deformation for the EBBTF with two plastic hinges developed in the two ends of the link is shown in Fig. 4(b), aiming at the derivation of the relationship between the inter-story drift angle θ and the inelastic link rotation angle γ_p.

The relationship between the inter-story drift angle θ and the inelastic link rotation angle γ_p is obtained as the Eq. (11)

$$\theta a=\theta\left(L\sin\alpha\right)=\gamma_p e \tag{11}$$

It is evident that the inelastic link rotation angle γ_p is mainly affected by the coefficient e/a, similar to the eccentricity ratio of traditional EBFs [18], which will quiet increase the ratio of link ductility measure to structure ductility measure as the length of shear link is always short.

4. Experimental Study

4.1 Specimen Descriptions

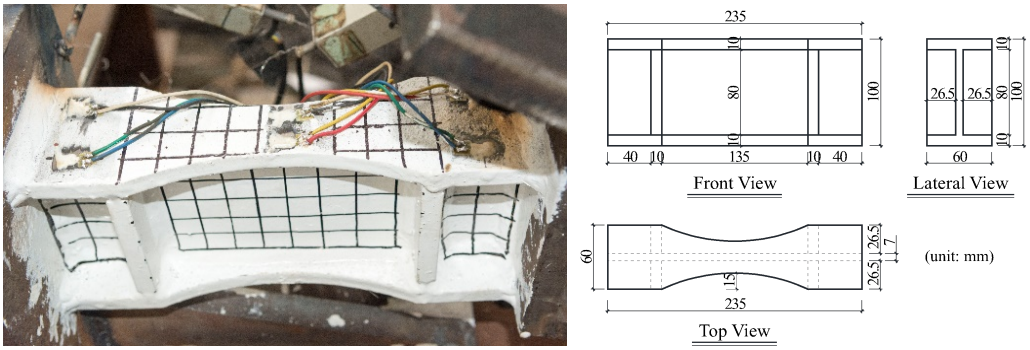

Fig. 5 – Configuration of short link with "dog-bone" flange

A total of seven eccentric bracing specimens were tested, and these specimens differ in three kinds of structural features, including the angle of brace, length of links and section feature of links. All of the seven eccentric bracing specimens were composed of welded H-section columns, cold-formed square-tube braces and welded H-section links of the same sectional dimensions, forming the lateral force-resisting system of the EBFs. And the sectional dimensions of the columns, braces and links were 125×125×6.5×9 mm, 100×12 mm and 100×60×10×8 mm respectively. Although the sectional dimensions of links in different specimens were identical, there were still four specifications of links designed considering the difference of length and section feature, and these specifications represent short link with regular flange, intermediate link with regular flange, long link with regular flange and short link with "dog-bone" flange, respectively. The short link with "dog-bone" flange is shown as Fig. 5. Full-depth intermediate stiffeners with thickness of 10 mm were welded to the webs and flanges of links under reasonable spacings to avoid web buckling as per GB50010-2010 [19]. A summary of these specimens is given in Table 1.

Table 1 – Details of test specimens

Specimen ID	Bracing feature	Link features		
	Angle α (°)	Length e (mm)	Length ratio $\rho=e/(M_p/V_p)$	Link section
L235-A16	16	235	1.3	Regular
L395-A16	16	395	2.2	Regular
L555-A16	16	555	3.1	Regular
L235- A22	22	235	1.3	Regular
L235- A22-R	22	235	1.3	"Dog-Bone"
L235- A30	30	235	1.3	Regular
L235- A30-R	30	235	1.3	"Dog-Bone"

4.2 Test Setup

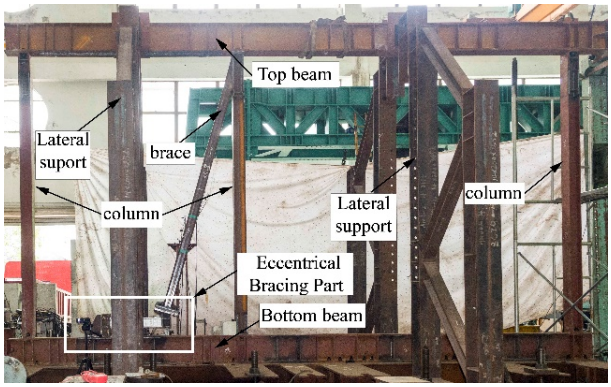

Fig. 6 – Photo of test setup

The test setup shown in Fig. 6 was developed. All specimens were fabricated and tested in the same full-scale one-story two-bay beam-through frame, where the dimensions of the welded H-section through beam and the welded H-section column were 300×150×10×12 mm and 125×125×6.5×9 mm respectively. The tested EBBTF is 3.34 m high from the centerline of the bottom through beam to the centerline of the top through beam, 3.34 m wide in the east bay and 2.28 m wide in the west bay. Forced displacement was applied by a 200t capacity computer-controlled servo actuator quasi-statically to the frame via the east side of top through beam. For preventing the top through beam from deflecting out-of-plane, lateral supports were provided on both sides of the middle of both west and east bays.

4.3 Loading Protocol

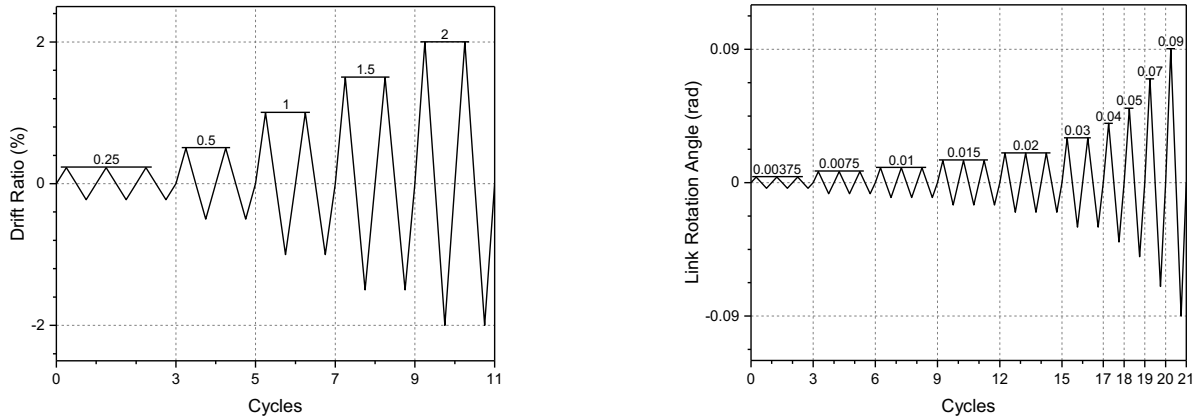

(a) Loading scheme of controlling story drift ratio (b) Loading scheme of controlling link rotation angle

Fig. 7 – Loading history

With reference to ANSI/AISC 341-10 [17], the applied displacement for the cyclic tests was controlled by the target story drift ratio history or link rotation history shown in Fig. 7. While the firstly tested specimen L235-A22 was controlled by the target story drift ratio history (see Fig. 7(a)) that would skip several link rotation levels, the target link rotation history (see Fig. 7(b)) was applied to the rest specimens with the aims to particularly investigate the ductility of the links under different link rotation angles. The tests were carried out until the complete failure of the specimens.

4.4 Material Properties

It was designed that the links were made of Q235B structural steel with a nominal yield stress of 235 MPa while other components were made of Q345B structural steel with a nominal yield stress of 345 MPa. Owing to the plasticity concentrated on the structural fuses, standard test coupons were only taken from the webs and flanges of the links. Average values of tensile yield stress, ultimate tensile stress and failure strain of the steels used in links are summarized as Table 2.

Table 2 – Material Properties

Components	Tensile yield stress f_y (MPa)	Ultimate tensile stress f_u (MPa)	Failure strain (%)
Link-flange	317	428	30%
Link-web	336	470	28%

5. Test results and discussions

5.1 General results

As the plastic deformation was intended to concentrate in the structural fuses, no visible damage occurred in the through beams and columns, and no plastic strain was detected in the braces. This also confirms that the repeated use of the boundary frame had limited influence on the test results. The main test results and fundamental behaviour of the considered specimens are summarized in Table 3. Note, as the hysteretic behaviour is symmetric, the test results given in the table are taken from the typical structural response under positive loading.

Table 3 – Summary of test results

Specimen ID	Theoretical elastic stiffness K_0(kN/mm)	Experimental elastic stiffness $K_{0,ex}$(kN/mm)	Yield load P_y (kN)	Ultimate load P_{max} (kN)	Ultimate inter-story drift ratio θ(%)	Ultimate link rotation angle γ(rad)
L235-A16	4.63	4.29	55	111	1.85	0.066
L395-A16	2.53	2.19	50	62.7	1.33	0.032
L555-A16	1.94	1.82	45.4	58.5	1.26	0.019
L235- A22	8.08	6.33	82.5	126	1.12	0.048
L235- A22-R	8.08	6.42	80	127	1.77	0.084
L235- A30	14.39	12.68	83.7	138	1.16	0.080
L235- A30-R	14.39	12.83	84.9	149	1.20	0.083

5.2 Test phenomena and failure mode

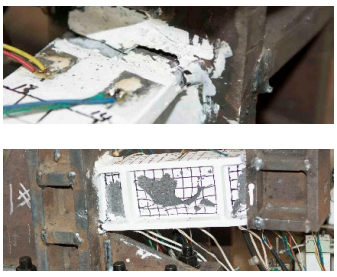

(a) Weld fractures

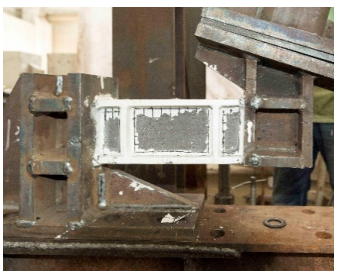

(b) Whitewash peeled off

(c) Weld defects

Fig. 8 – Test phenomena and failure mode

The cracks of all the specimens were initiated from the welds at the link ends and partially propagated to the adjacent web, as illustrated in Fig. 8(a). No signs of web buckling, flange buckling, or local instabilities were observed. Peeling-off of the link web whitewash occurred (displayed in Fig. 8(b)) which

confirmed the development of plasticity in the link webs. In some specimens, e.g., L235-A22-R, weld defects such as slag inclusions and weld porosity were observed (see Fig. 8(c)) when the weld region was separated from the link ends.

5.3 Comparative analysis

To investigate the effects of different testing parameters, a comparative study based on the obtained cyclic curves, ultimate lateral load capacities, stiffness, energy dissipation and ductility, was carried out. Note, this comparative analysis focuses on the hysteretic responses of the specimens before the initiation of critical cracking.

The areas of the last hysteresis cycle for different story drifts in the cyclic frame response curves are calculated to evaluate the hysteretic energy E_{hyst} dissipated in frame with different specimens. The equivalent stiffness K_{eff} is an important characteristic for performance assessment of frame in cyclic tests, and is determined with Eq. (12),

$$K_{eff} = \left(\left|P^{+}\right| + \left|P^{-}\right|\right) \Big/ \left(\left|\delta^{+}\right| + \left|\delta^{-}\right|\right) \tag{12}$$

where P^{+}, P^{-}, $\delta^{+}$and δ^{-} are the peak values of the lateral force and story drift of frame under positive and negative loadings.

5.3.1 Length of link

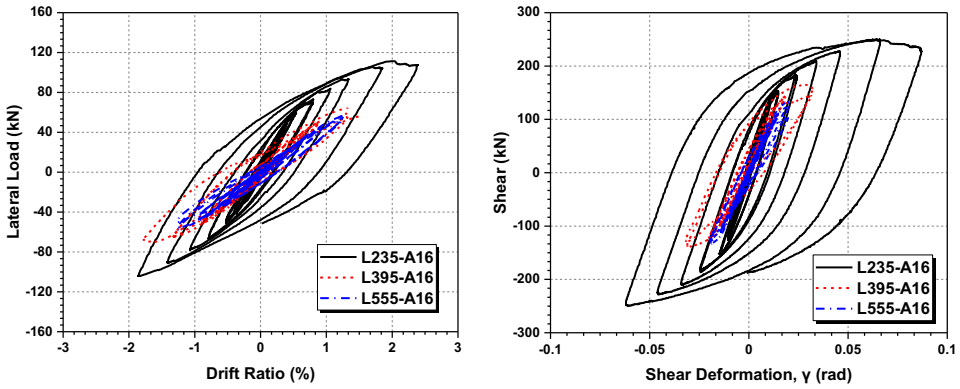

(a) Response of frame (b) Response of link

Fig. 9 – Experimental hysteretic curves of specimens with different link length

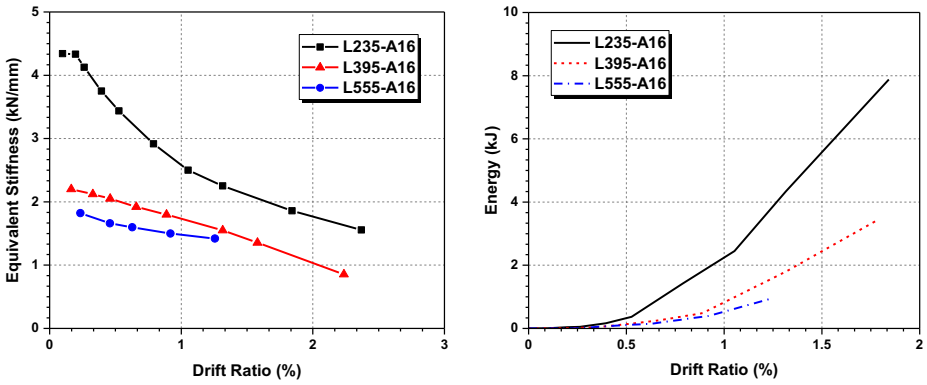

(a) Deterioration of equivalent stiffness (b) Energy dissipation under different drift ratio

Fig. 10 – Stiffness and energy dissipation of specimens with different link lengths

As shown in Fig. 9, the different ultimate story drift ratios of specimens L235-A16, L395-A16 and L555-A16 reflect the effect of the link length on the failure initiation and ductility performance of the link beams. Longer links resulted in larger end moment of links and higher stress concentration inside the weld

regions which led to earlier brittle weld fracture and premature specimen failure, thus length of links deeply influence the ductility of links and short links are preferable. With differences of link stiffness, the experimental elastic stiffness of the whole frame applied with specimens L235-A16, L395-A16 and L555-A16 slightly varied and the frame installed with the shortest link possessed the highest initial stiffness of 4.29 kN/mm. Fig. 10(a) demonstrates the deterioration of the equivalent stiffness response with increasing drift ratio and confirms that specimen L235-A16 with the shortest link always has the largest stiffness. The shear-dominated behavior exhibited in the link of specimen L235-A16 actually signifies plasticity development in entire link webs, which was experimentally perceived through the large area of painting peeled from the link webs. With the impact of flexure behavior, links of specimens L395-A16 and L555-A16 performed limited plasticity in link ends and insufficiency of energy dissipation with the comparison shown in Fig. 10(b).

5.3.2 Angle of brace

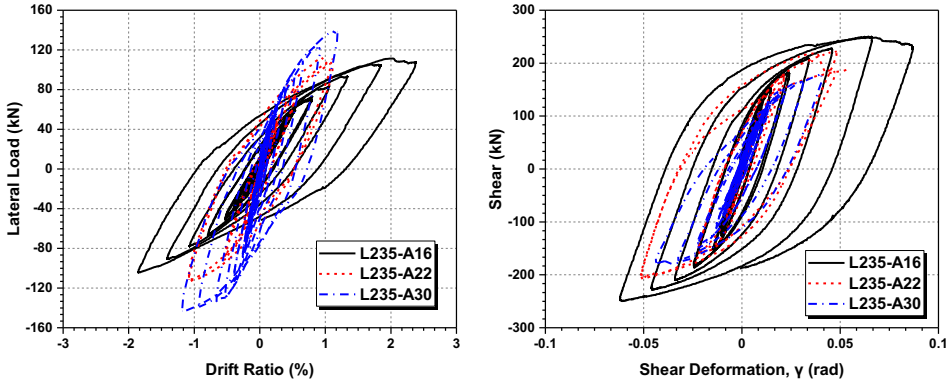

(a) Response of frame (b) Response of link

Fig. 11 – Experimental hysteretic curves of specimens with different bracing angle

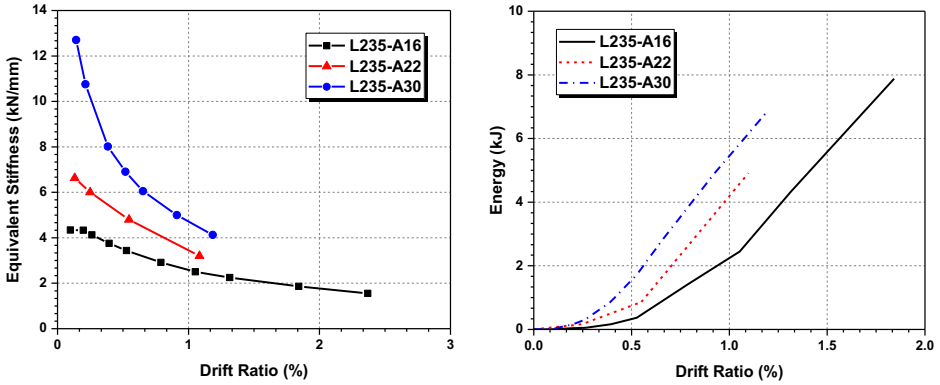

(a) Deterioration of equivalent stiffness (b) Energy dissipation under different drift ratio

Fig. 12 – Stiffness and energy dissipation of specimens with different bracing angle

Fig. 11 shows the hysteretic responses of specimens L235-A16, L235-A22 and L235-A30 with varying bracing angles. With a larger bracing angle, the horizontal projection of the brace *a* is increased and the *e*/*a* ratio is decreased. Therefore, according to the observed peak strength and stiffness (Fig. 12(a)), a substantial improvement in stiffness and strength can be achieved with decreasing *e*/*a* ratios. However, considering the relationship between the inter-story drift ratio and plastic link rotation angle (Eq. (11)), enlarging the bracing angle and decreasing the *e*/*a* ratio increase the ductility demand of the link. As shown in Fig. 11(b), weld fracture was initiated earlier in the specimen with a larger bracing angle, indicating lower ductility of the links. The reason behind the earlier weld fracture is the enlarged end moment in the link. Under the same inter-story drift, the inelastic link rotation angle is amplified with an increase in the bracing angle, resulting in more energy dissipation. Therefore, more energy is dissipated in specimens L235-A30 and

L235-A22 than specimen L235-A16 at small drift ratios, as shown in Fig. 12(b), although the total energy dissipation of specimen L235-A16 is the largest and exhibited the highest ductility.

5.3.3 Section geometry of link

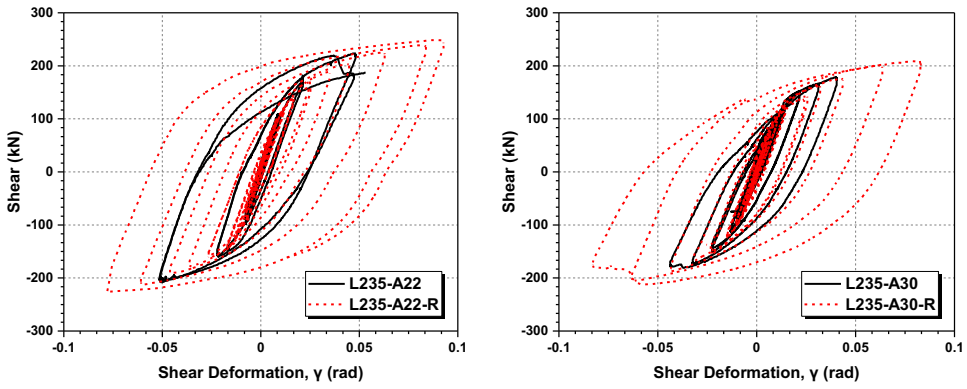

(a) (b)

Fig. 13 – Experimental hysteretic curves and envelope curves of links in specimens with different link section: (a) hysteretic curves of links in specimens L235-A22 and L235-A22-R (b) hysteretic curves of links in specimens L235-A30 and L235-A30-R

In contrast to specimens L235-A22 and L235-A30 with regular shear links, the flanges of the links of specimens L235-A22-R and L235-A30-R were trimmed to a “dog-bone” shape. It can be seen from Table 3 that the reduced link section barely affects the elastic stiffness and yield resistance of the system. Before the initiation of the weld cracks, the hysteretic responses of the reduced-section links were quite similar to that of the regular links, as shown in Fig. 13. With trimmed flanges, the stress concentration decreased, and the reduced-section links effectively delayed the weld fracture at the link ends and greatly enhanced the energy dissipation. Owing to the postponed weld failure, the reduced-section links were more ductile, enabling more pronounced plasticity developed in the link webs. This is also illustrated by more noticeable peeling-off of the whitewash for specimens L235-A22-R and L235-A30-R.

6. Conclusions

Seven full-scale specimens with different structural parameters were designed and tested. Major conclusions based on the observations and comparative analysis resulting from experiments are summarized as follows:

- Specimens of eccentrical braces with effective links enhanced the structural performance of beam-through steel frame structures with stable energy dissipation mechanism and sufficient stiffness.
- With plastic deformations and failures concentrated on the replaceable components of specimens, the through beams, columns and braces of the main frame remained undamaged state during the cyclic tests and the repeatable tests in the same BTF validated the post-earthquake rehabilitation of the new seismic systems.
- Short links with shear-dominant behaviors exhibited better performance in terms of stiffness, capacity and ductility compared with intermediate and long links in this lateral force-resisting system.
- Enlarging bracing angle, the stiffness and capacity of EBBTFs will be increased while the decreased ductility capacity of links may not meet with the higher ductility demand, which needs to be carefully considered in design.
- Weld fractures of link ends can be postponed to ensure adequate plasticity development with the application of flange-reduced links and resulting in no significant difference of cyclic responses before cracks initiation.

7. Acknowledgements

- The financial support from the National Natural Science Foundation of China (NSFC) with Grant Nos. 51778459 and 51820105013 are gratefully acknowledged.

8. References

[1] Wang, W., Zhou, Q., Chen, Y., Tong, L., & Chan, T. M. (2013): Experimental and numerical investigation on full-scale tension-only concentrically braced steel beam-through frames. *Journal of Constructional Steel Research*, 80, 369-385.

[2] Wang, W., Du, X., Zhang, Y., & Chen, Y. (2017): Experimental investigation of beam-through steel frames with self-centering modular panels. *Journal of Structural Engineering*, 143(5), 04017006.

[3] Wang, W., Kong, J., Zhang, Y., Chu, G., & Chen, Y. (2017): Seismic behavior of self-centering modular panel with slit steel plate shear walls: experimental testing. *Journal of Structural Engineering*, 144(1), 04017179.

[4] Azad, S. K., & Topkaya, C. (2017): A review of research on steel eccentrically braced frames. *Journal of constructional steel research*, 128, 53-73.

[5] Hjelmstad KD, Popov EP. (1983): Cyclic behavior and design of link beams. *Journal of Structural Engineering*, 109, 2387–403.

[6] Kasai K, Popov EP. (1986): General Behavior of WF steel shear link beams. *Journal of Structural Engineering*, 112, 362–82.

[7] Engelhardt MD, Popov EP. (1992): Experimental performance of long links in eccentrically braced frames. *Journal of Structural Engineering*, 118, 3067–88.

[8] Fussell AJ, Cowie KA, Clifton GC, Mago N. (2014): Development and research of eccentrically braced frames with replaceable active links. *Proc 2014 NZSEE Conf*, 1–10.

[9] Mansour N, Christopoulos C, Tremblay R. (2011): Experimental validation of replaceable shear links for eccentrically braced steel frames. *Journal of Structural Engineering*, 137, 1141–52.

[10] Kasai K, Popov EP. (1986): Cyclic Web buckling control for shear link beams. *Journal of Structural Engineering*, 112, 505–23.

[11] Dusicka P, Itani AM, Buckle IG. (2010): Cyclic behavior of shear links of various grades of plate steel. *Journal of Structural Engineering*, 136, 370–8.

[12] Okazaki T, Arce G, Ryu H-C, Engelhardt MD. (2005): Experimental study of local buckling, overstrength, and fracture of links in eccentrically braced frames. *Journal of Structural Engineering*, 131, 1526–35.

[13] Ramadan, T., & Ghobarah, A. (1995): Behaviour of bolted link-column joints in eccentrically braced frames. *Canadian Journal of Civil Engineering*, 22(4), 745-754.

[14] Okazaki T, Engelhardt MD. (2007): Cyclic loading behavior of EBF links constructed of ASTM A992 steel. *Journal of Constructional Steel Research*, 63, 751–65.

[15] Berman JW, Okazaki T, Hauksdottir HO. (2010): Reduced link sections for improving the ductility of eccentrically braced frame link-to-column connections. *Journal of Structural Engineering*, 136, 543–53.

[16] Stephens MT, Dusicka P, Lewis G. (2018): End web stiffeners for connecting ductile replaceable links. *Journal of Constructional Steel Research*, 150, 405–14.

[17] ANSI/AISC 341-10 (2010). Seismic provisions for structural steel buildings. Chicago, *American Institute of Steel Construction*.

[18] Hjelmstad KD, Popov EP. (1984): Characteristics of eccentrically braced frames. *Journal of Structural Engineering*, 110:340–53.

[19] GB 50011-2010 (2016). Code for seismic design of buildings. Beijing, China Architecture & Building Press, (in Chinese).

